Implications of the Observed Relationship between Tropical Cyclone Size and Intensity over the Western North Pacific

LIGUANG WU, WEI TIAN, QINGYUAN LIU, AND JIAN CAO

Pacific Typhoon Research Center and Key Laboratory of Meteorological Disaster of Ministry of Education, University of Information Science and Technology, Nanjing, China

JOHN A. KNAFF

NOAA Center for Satellite Applications and Research, Fort Collins, Colorado

(Manuscript received 1 September 2015, in final form 29 October 2015)

ABSTRACT

Tropical cyclone (TC) size, usually measured with the radius of gale force wind (34 kt or 17 m s^{-1}), is an important parameter for estimating TC risks such as wind damage, rainfall distribution, and storm surge. Previous studies have reported that there is a very weak relationship between TC size and TC intensity. A close examination presented here using satellite-based wind analyses suggests that the relationship between TC size and intensity is nonlinear. TC size generally increases with increasing TC maximum sustained wind before a maximum of 2.50° latitude at an intensity of 103 kt or 53.0 m s^{-1} and then slowly decreases as the TC intensity further increases. The observed relationship between TC size and intensity is compared to the relationships produced by an 11-yr seasonal numerical simulation of TC activity. The numerical simulations were able to produce neither the observed maximum sustained winds nor the observed nonlinear relationship between TC size and intensity. This finding suggests that TC size cannot reasonably be simulated with 9-km horizontal resolution and increased resolution is needed to study TC size variations using numerical simulations.

1. Introduction

Billions of people in Asian countries and Pacific islands are affected by tropical cyclones (TCs) or typhoons that form over the western North Pacific (WNP) and the South China Sea and thus mitigation of typhoon risks is an important task for governments in the region. Observational studies have suggested that TC size varies with season, region, latitude, environmental pressure, track type, and even the time of the day (Kimball and Mulekar 2004; Moyer et al. 2007; Lee et al. 2010). It is also found that the TC size may be affected by the synoptic environmental conditions (Merrill 1984; Holland and Merrill 1984; Weatherford and Gray 1988a; Cocks and Gray 2002; Liu and Chan 2002) along with eyewall dynamics (Maclay et al. 2008). Since TC size is an important parameter for determining TC impacts such as wind damage, rainfall distribution, storm surge, and ocean upwelling (Price 1981; Iman et al. 2005; Irish et al. 2008; Lin et al. 2015; Knaff and Sampson 2015), growing attention has been paid to the study of TC size. Previous studies have focused on the climatology of TC size with satellite products (e.g., Liu and Chan 2002; Kimball and Mulekar 2004; Kossin et al. 2007; Hill and Lackmann 2009; Chavas and Emanuel 2010; Knaff et al. 2014b; Chan and Chan 2015) and mechanisms that control TC size (Wang 2009; Xu and Wang 2010a,b; Fudeyasu and Wang 2011; Smith et al. 2011; Carrasco et al. 2014; Xu and Wang 2015; Kilroy et al. 2015).

While TC size has been measured with various parameters such as the radii of maximum wind (RMW), gale-force wind (34 kt or 17 m s^{-1}), damaging-force wind (50 kt or 25.7 m s^{-1}), hurricane-force wind (64 kt or 33 m s^{-1}), and the outmost closed isobar due to the availability of observational data (Merrill 1984; Weatherford and Gray 1988a,b; Kimball and Mulekar 2004; Moyer et al. 2007; Knaff et al. 2007; Maclay et al. 2008), the radius of gale-force wind (hereinafter R34) has been widely used due to

Corresponding author address: Prof. Liguang Wu, Pacific Typhoon Research Center, Key Laboratory of Meteorological Disaster, Ministry of Education, Nanjing University of Information Science and Technology, Nanjing 210044, China.
E-mail: liguang@nuist.edu.cn

DOI: 10.1175/JCLI-D-15-0628.1

its importance in determining TC potential impacts (Chan and Chan 2014; Knaff and Sampson 2015; Chan and Chan 2015). Although previous studies suggested that TC wind speed in the outer region was weakly related to TC intensity (Weatherford and Gray 1988b; Chan and Chan 2012), Knaff and Sampson (2015) suggested that with improved intensity forecasts the R34 forecast is also expected to improve. As one of the objectives of this study, we will examine the relationship between R34 and TC intensity in the western North Pacific basin using the Multiplatform Tropical Cyclone Surface Wind Analysis (MTCSWA; Knaff et al. 2011) data, which is the only high-resolution storm-centered wind dataset for individual TCs in the world.

Atmospheric general circulation models (AGCMs) have been an important tool for investigating the possible climate change of TC activity since Manabe et al. (1970) noticed for the first time that AGCMs were able to simulate some features of TC activity. Model horizontal grids for assessing the impacts of global warming on TC activity can be in the range of 10–50 km (Stowasser et al. 2007; Zhao et al. 2009; Caron et al. 2011; Murakami and Wang 2010; Murakami et al. 2011; Murakami et al. 2012; Manganello et al. 2012). Recently Kim et al. (2014) simulated global TC activity using the Geophysical Fluid Dynamics Laboratory (GFDL) Climate Model, version 2.5, which is a fully coupled global climate model with a horizontal resolution of about 50 km for the atmosphere and 25 km for the ocean. They suggested that TC size will increase by about 12% in response of CO_2 doubling. Given increasing horizontal resolutions of climate system models, the other objective of this study is to examine the capability of a high-resolution climate model in simulating TC size.

2. R34 data

a. MTCSWA

The MTCSWA is created for each TC using only satellite-based information (Knaff et al. 2011). The dataset contains the storm-centered one-minute surface and flight-level (~700 hPa) wind fields from 2007 onward. The 6-h gridded wind fields have a horizontal resolution of 0.1° latitude by 0.1° longitude. Using Hurricane Wind Analysis System (H*Wind) analyses as ground truth in the Atlantic basin, the MTCSWA winds are shown to have mean absolute errors (MAEs) less than 5 m s^{-1} over most of a 400 km × 400 km domain centered on TCs (Knaff et al. 2011). The MTCSWA data are produced for real-time use, and the storm intensity and location are estimated from the most recent operational estimates and forecast (Knaff et al. 2011). In this study, 2022 observations for 128 TCs that occurred in the WNP basin during the period 2007–13 are available (Fig. 1, top).

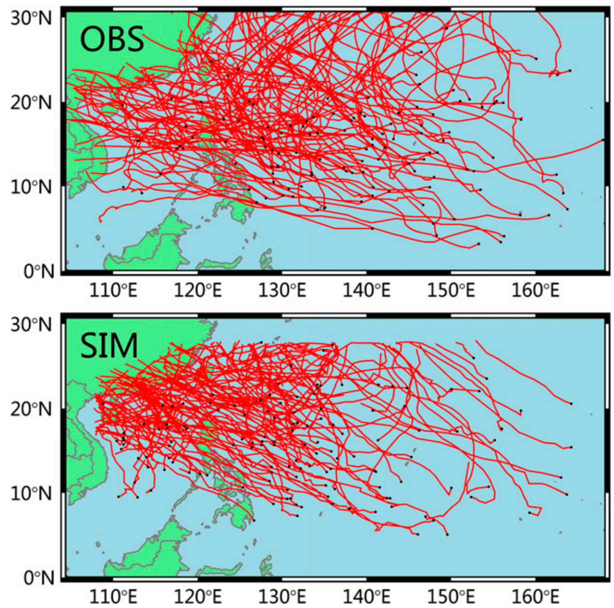

FIG. 1. TC tracks within the second model domain: (top) observed during the period 2007–13 and (bottom) simulated in the peak season (July–September) of 2000–10.

b. Numerical experiments

The full-physics WRF Model has been widely used in simulating individual TCs and TC climatology (e.g., Davis et al. 2008; Jin et al. 2013; Kim et al. 2015). To examine the skill of dynamics models in the intraseasonal prediction of TC activity, Cao et al. (2012) used the version 3.0 of the WRF Model and simulated TC activity in the peak season (July–September) during 2000–10. Two interactive model domains are used with 38 vertical levels with a model top of 50 hPa. The coarse domain covers the region of 20°S–60°N, 96°E–166°W with a horizontal resolution of 27 km. The 9-km nesting domain contains 691 × 355 grid points, covering the region of 0°–31°N, 104°E–168.5°W (Fig. 1, bottom). For each year, the model was initiated at 0000 UTC 1 July with the initial and lateral boundary conditions from the National Centers for Environmental Prediction (NCEP) final operational global analysis (FNL) with 1° × 1° latitude–longitude grids at 6-h intervals and terminated at 1200 UTC 30 September. The analysis nudging for the wind components above the lower boundary layer is used in the outer domain to force the simulated large-scale patterns close to the observation. The nudging coefficient is set to 1.5×10^{-4} s^{-1}. In this study, we only use the TC wind data in the 9-km nesting domain.

A TC simulated in the 9-km domain is defined if 1) there is a closed isobar with the minimum surface pressure lower than 1000 hPa, 2) the maximum wind speed at 10 m exceeds tropical storm intensity (17.2 m s^{-1}) within a radius of 360 km from the center, 3) a warm core appears between 500 and 300 hPa, and 4) its lifetime lasts at least 48 h. A variational approach is used to locate the TC center until the maximum azimuthal mean tangential wind speed is obtained (Wu et al. 2006).

During the 11-yr period (2000–10), the JTWC best-track data recorded 144 TCs in the peak season over the WNP and South China Sea and 138 of them formed in the 9-km domain, accounting for 96% of the TCs observed in the basin. In the 11-season simulation, 152 TCs are identified in the 9-km domain. Close inspection of the simulated TCs indicates that the azimuthal mean wind speed of 16 TCs never reaches the tropical storm intensity (34 kt) during their lifetime. For this reason, these TCs are excluded for the analysis and thus the wind data of the 136 simulated TCs are used in the subsequent analysis (Fig. 1, bottom). We can see that the simulated TC tracks do not reach the northern boundary since the detection algorithm for TC centers requires a minimum distance of 360 km.

We further examined the frequency distribution of the simulated TC intensity in terms of maximum sustained wind speed (not shown). The simulated TCs show a single intensity peak of category 2 with no category 4 and 5 TCs. (The TC categories are based on the Saffir-Simpson scale.) This intensity distribution of the simulated TCs is similar to that in Kim et al. (2015). Our simulation suggests that a horizontal resolution of 9 km × 9 km is still too coarse for realistically simulating the intensity distribution. Gentry and Lackmann (2010) used the WRF Model to test the sensitivity of simulations of Hurricane Ivan (2004) to different horizontal model resolution. Chen et al. (2007) and Fierro et al. (2009) suggested that grid spacing of 2 km or less is needed for representation of important physical processes in the TC eyewall.

3. Relationship between R34 and TC intensity in the MTCSWA

Figure 2a shows the scatter diagram of the R34 in the MTCSWA data, in which the mean R34 is 1.81° latitude with a standard deviation of 1.02°. The mean R34 is smaller than the mean R34 in Knaff et al. (2007) and Chan and Chan (2012). Knaff et al. (2007) used the operational wind radii estimates during the period 1988–2003 and found that the mean R34 was 1.92° latitude for the WNP basin. Using the 10-yr (1999–2009) QuikSCAT data, Chan and Chan (2012) obtained a mean R34 of 2.13° latitude, which is larger than the mean R34 in the MTCSWA data and the estimate in Knaff et al. (2007).

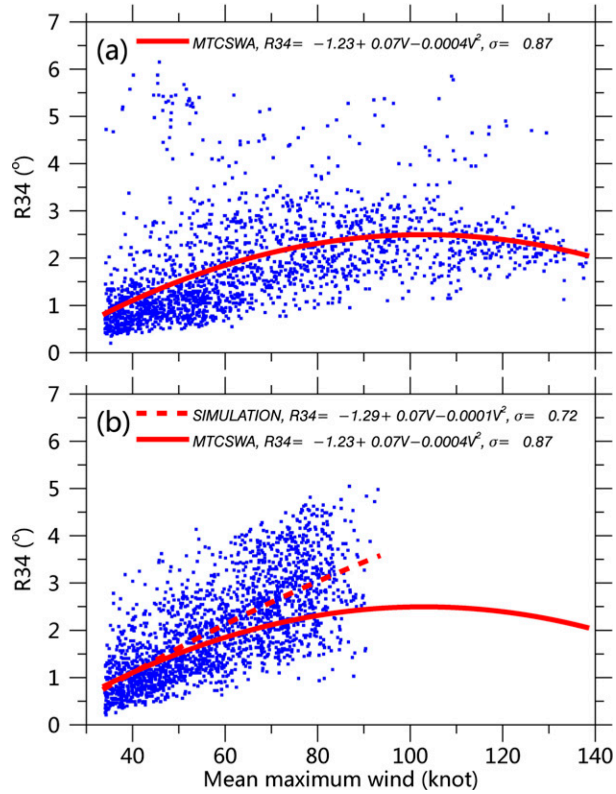

FIG. 2. Relationships between TC size (R34) and mean maximum wind speed from (a) MTCSWA and (b) simulation. The solid and dashed lines show the fitting curves for observation and simulation, respectively.

Considering the different datasets, time periods, and uncertainty in the R34 datasets, we think that the mean R34 in the MTCSWA data is in general comparable to these previous studies.

The relationship between the TC size and intensity in the MTCSWA data can be fitted with the quadratic function of $R34 = -1.23 + 0.07V - 0.004V^2$, where V is the azimuthal mean of the one-minute TC maximum wind in knots (kt; 1 kt ≈ 0.51 m s^{-1}). The fitting curve suggests that R34 has a maximum of 2.50° latitude in the MTCSWA data at 103 kt. This shape is also similar to the mean size distribution produced from the datasets of Knaff et al. (2014b) as presented in Knaff et al. (2014a, their Fig. 3). The R34 generally increases with increasing TC intensity before reaching the maximum and slightly decreases with further intensity increase. Although R34 can vary widely at certain intensity, Fig. 2a suggests that there is, in an average sense, an upper limit (2.50° latitude) for R34 in the western North Pacific basin.

Note that some samples show a R34 larger than 3.85° latitude (two standard deviations) in Fig. 2a. We examine all the 96 samples and found that most of these samples (82.3%) were associated with low-frequency

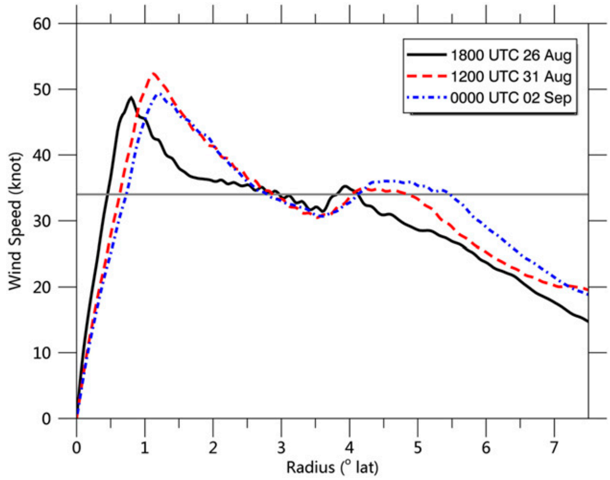

FIG. 3. The 700-hPa radial wind profile of Tropical Storm Talas (2011) with a second wind maximum between 4° and 5° latitude radius.

monsoon gyres or cyclonic circulations. Monsoon gyres are a specific pattern of the evolution of low-level monsoon circulation and can be identified as a low-frequency, nearly circular cyclonic vortex with a diameter of about 2500 km (Lander 1994; Wu et al. 2011a,b; Wu et al. 2013). The radial wind profile of Tropical Storm Talas (2011) is a typical example for the large R34 cases (Fig. 3), which accounts for 24 of the 96 samples. During the period from 1800 UTC 26 August to 0000 UTC 2 September, there is a second maximum in the azimuthal mean wind 400–600 km away from the TC center. We examine the 850-hPa wind fields associated with Tropical Storm Talas in the NCEP FNL data with 1° × 1° latitude–longitude grids at 6-h intervals. We found that a low-frequency cyclonic circulation was collocated with the TC (figure not shown), which can lead to the second maximum in the azimuthal mean wind 400–600 km away from the TC center in Fig. 3. Wu et al. (2013) found that 19.8% of TC formation events were associated with monsoon gyres in May–October during 2000–10.

4. Relationship between R34 and TC intensity in the simulation

We further examine the simulated R34 data. The simulated sample size for R34 is 2058 and the mean R34 is 2.02° latitude with a standard deviation of 1.02°. Figure 2b shows the scatter diagram of the R34 and TC intensity in the WRF simulation. Note that there are no samples beyond the intensity of 93 kt. The relationship between the TC size and intensity can also be fitted with the quadratic function of $R34 = -1.29 + 0.07V - 0.0001V^2$. From the fitting curve, we can see that the simulated R34 generally increases with increasing TC intensity, in agreement with the relationships derived from the MTCSWA data. As the TC intensity increases in the simulation, the simulated R34 becomes larger than that in the observation. We speculate that the difference may be due to the relatively coarse model resolution that cannot well resolve the TC wind distribution in the radial direction as TC intensity increases. Because of the relationship between TC size and intensity, it is suggested that improvement in the simulation of TC size depends upon the improvement in the simulation of TC intensity, in agreement with Knaff and Sampson (2015). Note that the model can simulate the central pressure as low as the observation, but the model has difficulty in simulating the observed nonlinear relationship between the TC size and the central pressure.

In previous studies, it has been suggested that the correlation between TC size and intensity is low (Merrill 1984; Weatherford and Gray 1988b; Chan and Chan 2012). In addition to uncertainty in R34 datasets, we think the low correlation may also due to the nonlinear relationship. For this reason, we calculate the correlations between the R34 and TC intensity for the samples with intensity less than 93 kt and R34 less than 3.85° latitude (two standard deviations). In this case, the correlations are 0.71 in the simulation and 0.64 in the MTCSWA data, suggesting a statistically significant relationship between TC intensity and TC size.

5. Summary

TC size, usually measured with the radius of gale-force wind, is an important parameter for estimating TC risks. While the climatology of TC size is well established, a statistical relationship is derived between TC size and intensity in the WNP basin from the MTCSWA data in this study. Although it can largely vary due to the presence of monsoon gyres in the western North Pacific basin, TC size increases with increasing TC maximum sustained wind before a maximum of 2.50° latitude at the intensity of 103 kt or 53.0 m s^{-1} and then it slowly decreases as the TC intensity further increases, suggesting an upper limit for R34 or TC size. Gray (1998) suggested that tropical disturbances cannot intensify over the entire region instantaneously, but it is more efficient for the disturbance to intensify in a limited area. We think that the argument may be also suitable for TC intensification. The observed relationship between TC size and intensity is also examined in the seasonal numerical simulation of 11-yr TC activity. The relationship cannot be reasonably simulated even with the model spacing of 9 km. The derived statistical relationship can be used in mitigation of TC risks and estimation of TC damage.

Acknowledgments. This research was jointly supported by the National Basic Research Program of China (2013CB430103, 2015CB452803), the National Natural Science Foundation of China (Grant 41275093), the project of the specially appointed professorship of Jiangsu Province, and the Natural Science Foundation for Higher Education Institutions in Jiangsu Province (15KJB170008). TC data and FNL data are from the JTWC and NCEP. The TC wind data were provided by Dr. John A. Knaff. The views, opinions, and findings contained in this report are those of the authors and should not be construed as an official National Oceanic and Atmospheric Administration or U.S. government position, policy, or decision.

REFERENCES

Cao, J., L. Wu, and W. Pan, 2012: Simulated seasonal activity of tropical cyclones over the western North Pacific during July–September 2006. *J. Nanjing Inst. Meteor.*, **35**, 148–162.

Caron, L.-P., C. G. Jones, and K. Winger, 2011: Impact of resolution and downscaling technique in simulating recent Atlantic tropical cyclone activity. *Climate Dyn.*, **37**, 869–892, doi:10.1007/s00382-010-0846-7.

Carrasco, C., C. Landsea, and Y. Lin, 2014: The influence of tropical cyclone size on its intensification. *Wea. Forecasting*, **29**, 582–590, doi:10.1175/WAF-D-13-00092.1.

Chan, K. T. F., and J. C. L. Chan, 2012: Size and strength of tropical cyclones as inferred from QuikSCAT data. *Mon. Wea. Rev.*, **140**, 811–824, doi:10.1175/MWR-D-10-05062.1.

——, and ——, 2014: Impacts of initial vortex size and planetary vorticity on tropical cyclone size. *Quart. J. Roy. Meteor. Soc.*, **140**, 2235–2248, doi:10.1002/qj.2292.

——, and ——, 2015: Global climatology of tropical cyclone size as inferred from QuikSCAT data. *Quart. J. Roy. Meteor. Soc.*, doi:10.1002/joc.4307, in press.

Chavas, D. R., and K. A. Emanuel, 2010: A QuikSCAT climatology of tropical cyclone size. *Geophys. Res. Lett.*, **37**, L18816, doi:10.1029/2010GL044558.

Chen, S. S., J. F. Price, W. Zhao, M. A. Donelan, and E. J. Walsh, 2007: The CBLAST-Hurricane Program and the next-generation fully coupled atmosphere–wave–ocean models for hurricane research and prediction. *Bull. Amer. Meteor. Soc.*, **88**, 311–317, doi:10.1175/BAMS-88-3-311.

Cocks, S. B., and W. M. Gray, 2002: Variability of the outer wind profiles of western North Pacific typhoons: Classifications and techniques for analysis and forecasting. *Mon. Wea. Rev.*, **130**, 1989–2005, doi:10.1175/1520-0493(2002)130<1989:VOTOWP>2.0.CO;2.

Davis, C., and Coauthors, 2008: Prediction of landfalling hurricanes with the Advanced Hurricane WRF Model. *Mon. Wea. Rev.*, **136**, 1990–2005, doi:10.1175/2007MWR2085.1.

Fierro, A. O., R. F. Rogers, F. D. Marks, and D. S. Nolan, 2009: The impact of horizontal grid spacing on the microphysical and kinematic structures of strong tropical cyclones simulated with the WRF–ARW model. *Mon. Wea. Rev.*, **137**, 3717–3743, doi:10.1175/2009MWR2946.1.

Fudeyasu, H., and Y. Wang, 2011: Balanced contribution to the intensification of a tropical cyclone simulated in TCM4: Outer-core spinup process. *J. Atmos. Sci.*, **68**, 430–449, doi:10.1175/2010JAS3523.1.

Gentry, M. S., and G. M. Lackmann, 2010: Sensitivity of simulated tropical cyclone structure and intensity to horizontal resolution. *Mon. Wea. Rev.*, **138**, 688–704, doi:10.1175/2009MWR2976.1.

Gray, W. M., 1998: The formation of tropical cyclones. *Meteor. Atmos. Phys.*, **67**, 37–69, doi:10.1007/BF01277501.

Hill, K. A., and G. M. Lackmann, 2009: Influence of environmental humidity on tropical cyclone size. *Mon. Wea. Rev.*, **137**, 3294–3315, doi:10.1175/2009MWR2679.1.

Holland, G. J., and R. T. Merrill, 1984: On the dynamics of tropical cyclone structural changes. *Quart. J. Roy. Meteor. Soc.*, **110**, 723–745, doi:10.1002/qj.49711046510.

Iman, R. L., M. E. Johnson, and C. C. Watson, 2005: Sensitivity analysis for computer model projections of hurricane losses. *Risk Anal.*, **25**, 1277–1297, doi:10.1111/j.1539-6924.2005.00673.x.

Irish, J. L., D. T. Resio, and J. J. Ratcliff, 2008: The influence of storm size on hurricane surge. *J. Phys. Oceanogr.*, **38**, 2003–2013, doi:10.1175/2008JPO3727.1.

Jin, C.-S., C.-H. Ho, J.-H. Kim, D.-K. Lee, D.-H. Cha, and S.-W. Yeh, 2013: Critical role of northern off-equatorial sea surface temperature forcing associated with central Pacific El Niño in more frequent tropical cyclone movements toward East Asia. *J. Climate*, **26**, 2534–2545, doi:10.1175/JCLI-D-12-00287.1.

Kilroy, G., R. K. Smith, and M. T. Montgomery, 2015: Why do model tropical cyclones grow progressively in size and decay in intensity after reaching maturity? Tropical Cyclone Research Rep. TCRR 2, Meteorological Institute, Ludwig Maximilians University of Munich, 16 pp.

Kim, D., C. S. Jin, C. H. Ho, J. Kim, and J. H. Kim, 2015: Climatological features of WRF-simulated tropical cyclones over the western North Pacific. *Climate Dyn.*, **44**, 3223–3235, doi:10.1007/s00382-014-2410-3.

Kim, H.-S., G. A. Vecchi, T. Knutson, W. G. Anderson, T. L. Delworth, A. Rosati, F. Zeng, and M. Zhao, 2014: Tropical cyclone simulation and response to CO_2 doubling in the GFDL CM2.5 high-resolution coupled climate model. *J. Climate*, **27**, 8034–8054, doi:10.1175/JCLI-D-13-00475.1.

Kimball, S. K., and M. S. Mulekar, 2004: A 15-year climatology of North Atlantic tropical cyclones. Part I: Size parameters. *J. Climate*, **17**, 3555–3575, doi:10.1175/1520-0442(2004)017<3555:AYCONA>2.0.CO;2.

Knaff, J. A., and C. R. Sampson, 2015: After a decade are Atlantic tropical cyclone gale force wind radii forecasts now skillful? *Wea. Forecasting*, **30**, 702–709, doi:10.1175/WAF-D-14-00149.1.

——, ——, M. DeMaria, T. P. Marchok, J. M. Gross, and C. J. McAdie, 2007: Statistical tropical cyclone wind radii prediction using climatology and persistence. *Wea. Forecasting*, **22**, 781–791, doi:10.1175/WAF1026.1.

——, M. DeMaria, D. A. Molenar, C. R. Sampson, and M. G. Seybold, 2011: An automated, objective, multiple-satellite-platform tropical cyclone surface wind analysis. *J. Appl. Meteor. Climatol*, **50**, 2149–2166, doi:10.1175/2011JAMC2673.1.

——, ——, S. Longmore, and R. T. DeMaria, 2014a: Improving tropical cyclone guidance tools by accounting for variations in size. *31st Conf. on Hurricanes and Tropical Meteorology*, San Diego, CA., Amer. Meteor. Soc., 51. [Available online at https://ams.confex.com/ams/31Hurr/webprogram/Paper244165.html.]

——, S. P. Longmore, and D. A. Molenar, 2014b: An objective satellite-based tropical cyclone size climatology. *J. Climate*, **27**, 455–476, doi:10.1175/JCLI-D-13-00096.1.

Kossin, J. P., J. A. Knaff, H. I. Berger, D. C. Herndon, T. A. Cram, C. S. Velden, R. J. Murnane, and J. D. Hawkins, 2007: Estimating hurricane wind structure in the absence of aircraft reconnaissance. *Wea. Forecasting*, **22**, 89–101, doi:10.1175/WAF985.1.

Lander, M. A., 1994: Description of a monsoon gyre and its effects on the tropical cyclones in the western North Pacific during August 1991. *Wea. Forecasting*, **9**, 640–654, doi:10.1175/1520-0434(1994)009<0640:DOAMGA>2.0.CO;2.

Lee, C.-S., K. K. W. Cheung, W.-T. Fang, and R. L. Elsberry, 2010: Initial maintenance of tropical cyclone size in the western North Pacific. *Mon. Wea. Rev.*, **138**, 3207–3223, doi:10.1175/2010MWR3023.1.

Lin, Y., M. Zhao, and M. Zhang, 2015: Tropical cyclone rainfall area controlled by relative sea surface temperature. *Nat. Commun.*, **6**, 6591, doi:10.1038/ncomms7591.

Liu, K. S., and J. C. L. Chan, 2002: Synoptic flow patterns associated with small and large tropical cyclones over the western North Pacific. *Mon. Wea. Rev.*, **130**, 2134–2142, doi:10.1175/1520-0493(2002)130<2134:SFPAWS>2.0.CO;2.

Maclay, K. S., M. DeMaria, and T. H. Vonder Haar, 2008: Tropical cyclone inner core kinetic energy evolution. *Mon. Wea. Rev.*, **136**, 4882–4898, doi:10.1175/2008MWR2268.1.

Manabe, S., J. L. Holloway, and H. M. Stone, 1970: Tropical circulation on a time integration of a global model of the atmosphere. *J. Atmos. Sci.*, **27**, 580–613, doi:10.1175/1520-0469(1970)027<0580:TCIATI>2.0.CO;2.

Manganello, J. V., and Coauthors, 2012: Tropical cyclone climatology in a 10-km global atmospheric GCM: Toward weather-resolving climate modeling. *J. Climate*, **25**, 3867–3893, doi:10.1175/JCLI-D-11-00346.1.

Merrill, R. T., 1984: A comparison of large and small tropical cyclones. *Mon. Wea. Rev.*, **112**, 1408–1418, doi:10.1175/1520-0493(1984)112<1408:ACOLAS>2.0.CO;2.

Moyer, A. C., J. L. Evans, and M. Powell, 2007: Comparison of observed gale radius statistics. *Meteor. Atmos. Phys.*, **97**, 41–55, doi:10.1007/s00703-006-0243-2.

Murakami, H., and B. Wang, 2010: Future change of North Atlantic tropical cyclone tracks: Projection by a 20-km-mesh global atmospheric model. *J. Climate*, **23**, 2699–2721, doi:10.1175/2010JCLI3338.1.

——, ——, and A. Kitoh, 2011: Future change of western North Pacific typhoons: Projections by a 20-km-mesh global atmospheric model. *J. Climate*, **24**, 1154–1169, doi:10.1175/2010JCLI3723.1.

——, and Coauthors, 2012: Future changes in tropical cyclone activity projected by the new high-resolution MRI-AGCM. *J. Climate*, **25**, 3237–3260, doi:10.1175/JCLI-D-11-00415.1.

Price, J. F., 1981: Upper ocean response to a hurricane. *J. Phys. Oceanogr.*, **11**, 153–175, doi:10.1175/1520-0485(1981)011<0153:UORTAH>2.0.CO;2.

Smith, R. K., C. W. Schmidt, and M. T. Montgomery, 2011: An investigation of rotational influences on tropical-cyclone size and intensity. *Quart. J. Roy. Meteor. Soc.*, **137**, 1841–1855, doi:10.1002/qj.862.

Stowasser, M., Y. Wang, and K. Hamilton, 2007: Tropical cyclone changes in the western North Pacific in a global warming scenario. *J. Climate*, **20**, 2378–2396, doi:10.1175/JCLI4126.1.

Wang, Y., 2009: How do outer spiral rainbands affect tropical cyclone structure and intensity? *J. Atmos. Sci.*, **66**, 1250–1273, doi:10.1175/2008JAS2737.1.

Weatherford, C. L., and W. M. Gray, 1988a: Typhoon structure as revealed by aircraft reconnaissance. Part I: Data analysis and climatology. *Mon. Wea. Rev.*, **116**, 1032–1043, doi:10.1175/1520-0493(1988)116<1032:TSARBA>2.0.CO;2.

——, and ——, 1988b: Typhoon structure as revealed by aircraft reconnaissance. Part II: Structural variability. *Mon. Wea. Rev.*, **116**, 1044–1056, doi:10.1175/1520-0493(1988)116<1044:TSARBA>2.0.CO;2.

Wu, L., S. A. Braun, J. Halverson, and G. Heymsfield, 2006: A numerical study of Hurricane Erin (2001). Part I: Model verification and storm evolution. *J. Atmos. Sci.*, **63**, 65–86, doi:10.1175/JAS3597.1.

——, J. Liang, and C.-C. Wu, 2011a: Monsoonal influence on Typhoon Morakot (2009). Part I: Observational analysis. *J. Atmos. Sci.*, **68**, 2208–2221, doi:10.1175/2011JAS3730.1.

——, H. Zong, and J. Liang, 2011b: Observational analysis of sudden tropical cyclone track changes in the vicinity of the East China Sea. *J. Atmos. Sci.*, **68**, 3012–3031, doi:10.1175/2010JAS3559.1.

——, Z. Ni, J. Duan, and H. Zong, 2013: Sudden tropical cyclone track changes over western North Pacific: A composite study. *Mon. Wea. Rev.*, **141**, 2597–2610, doi:10.1175/MWR-D-12-00224.1.

Xu, J., and Y. Wang, 2010a: Sensitivity of the simulated tropical cyclone inner-core size to the initial vortex size. *Mon. Wea. Rev.*, **138**, 4135–4157, doi:10.1175/2010MWR3335.1.

——, and ——, 2010b: Sensitivity of tropical cyclone inner core size and intensity to the radial distribution of surface entropy flux. *J. Atmos. Sci.*, **67**, 1831–1852, doi:10.1175/2010JAS3387.1.

——, and ——, 2015: A statistical analysis on the dependence of tropical cyclone intensification rate on the storm intensity and size in the North Atlantic. *Wea. Forecasting*, **30**, 692–701, doi:10.1175/WAF-D-14-00141.1.

Zhao, M., I. M. Held, S.-J. Lin, and G. A. Vecchi, 2009: Simulations of global hurricane climatology, interannual variability, and response to global warming using a 50-km resolution GCM. *J. Climate*, **22**, 6653–6678, doi:10.1175/2009JCLI3049.1.